

Regime for a self-ionizing Raman laser amplifier

Daniel S. Clark^{a)} and Nathaniel J. Fisch^{b)}

Plasma Physics Laboratory, Princeton University, P.O. Box 451, Princeton, New Jersey 08543

(Received 7 September 2001; accepted 28 February 2002)

Backward Raman amplification and compression at high power might occur if a long pumping laser pulse is passed through a plasma to interact resonantly with a counter-propagating short seed pulse [V. M. Malkin *et al.*, Phys. Rev. Lett. **82**, 4448–4451 (1999)]. One critical issue, however, is that the pump may be unacceptably depleted due to spontaneous Raman backscatter from intrinsic fluctuations in the amplifying plasma medium prior to its useful interaction with the seed. Premature backscatter may be avoided, however, by employing a gaseous medium with pump intensities too low to ionize the medium and using the intense seed to produce the plasma by rapid photoionization as it is being amplified [V. M. Malkin *et al.*, Phys. Plasmas **8**, 4698–4699 (2001)]. In addition to allowing that only rather low power pumps be used, photoionization introduces a damping of the short pulse which must be overcome by the Raman growth rate for net amplification to occur. The parameter space of gas densities, laser wavelengths, and laser intensities is surveyed to identify favorable regimes for this effect. Output laser intensities of 2×10^{17} W/cm² for 0.5 μ m radiation are found to be feasible for such a scheme using a pump of 1×10^{13} W/cm² and an initial seed of 5×10^{14} W/cm² over an amplification length of 5.6 cm in hydrogen gas. © 2002 American Institute of Physics. [DOI: 10.1063/1.1471515]

I. INTRODUCTION

Through the last several decades, applications such as inertial confinement fusion (ICF),¹ laser wake field particle acceleration,² or investigations of nonlinear quantum electrodynamics³ have driven the search for ever higher laser intensities in ever shorter pulses. In the mid-1980s the development of the chirped pulse amplification (CPA) technique enabled the remarkable increase in peak unfocused laser intensities from the then limit of $\sim 10^9$ W/cm² to the range of several 10^{12} W/cm².⁴ While the CPA technique has yielded tremendous advances in laser powers, access to yet higher powers and intensities by this process is frustrated by the requirement of impractically large diffraction gratings of the multi-meter scale and the fixed damage thresholds of these fragile, high-precision elements to ultrahigh light intensities. Nevertheless, such schemes as the fast ignitor for laser fusion (requiring ~ 1 ps pulses of $\sim 10^{20}$ W/cm² intensities)⁵ or studies of photon decay by electron–positron pair production (at intensities greater than 10^{30} W/cm²) demand powers at or beyond current limits of CPA and so motivate the search for yet more efficient as well as compact laser amplifiers capable of withstanding ultra-intense laser fluences. In this regard, the essential indestructibility of plasma under currently imaginable laser intensities particularly suggests its use as a laser amplifying element.

To meet such a need, a scheme has recently been proposed⁶ for the amplification of *unfocused* pulses into the 10^{17} W/cm² range using backward Raman scattering in plasma slabs. In this technique, a long laser “pump” pulse of large integrated energy is collided with a narrow, oppositely-

propagating “seed” pulse. The nonlinear evolution of the Raman scattering instability was found analytically to result in the scattering of the pump power into the narrow seed pulse with this backward propagating seed both amplifying and narrowing (compressing) linearly in time. A efficiency for energy transfer from the pump pulse to the seed of 80% should be possible with a focused seed intensity reaching on the order of 10^5 times what is currently achievable.

However, the stability of the pump pulse to spontaneous Raman backscatter from intrinsic fluctuations in the plasma medium, which could degrade or entirely suppress the amplification effect, is of concern. Stabilization of this unwanted Raman scattering of the pump pulse might be achieved by exploiting the nonlinear narrowing of the seed as it amplifies.⁷ Since the seed is rapidly narrowing in space during its nonlinear amplification, its consequent broadening in frequency renders this nonlinear amplification phase robust to “detuning” from the exact Raman resonance. The linear evolution of the premature backward scattering of the pump (during which any signal broadens as opposed to narrowing⁸), however, without such broad spectra, would not be resilient to such deviations from resonance. The introduction of a spatial variation in the plasma frequency (i.e., density) to detune the seed from forward scattering and an opposed temporal chirp of the pump pulse to detune from backscattering would then suppress these undesired scattering mechanisms. Analytical and numerical calculations in one dimension have shown this continued nonlinear amplification of the seed pulse in the presence of slight detuning.

This analysis was performed in the limit of a cold, collisionless fluid plasma without realistic modeling of spontaneous pump backscatter from plasma noise,⁹ however. Simulations with the particle-in-cell (PIC) code Zohar,¹⁰ in which the effect of discreteness-induced plasma noise is included,

^{a)}Electronic mail: dclark@pppl.gov

^{b)}Electronic mail: fisch@pppl.gov

suggest that such backscatter may be a significant concern. While the fluctuation level is significantly exaggerated in PIC codes relative to that in a real plasma (due to the far fewer particles per Debye sphere in any conceivable simulation compared to a realistic weakly coupled plasma¹¹), it remains to be demonstrated convincingly that a relatively high intensity laser pump may be propagated stably through ~ 1 cm of plasma of reasonable density for strong nonlinear coupling. The Raman amplification effect may be demonstrated in particle simulations using “cold” or “quiet” starts in which no fluctuations initially exist in the plasma, effectively a plasma of zero temperature; but such simulations, while including certain discrete-plasma effects, effectively sidestep the crucial question of pump stability to intrinsic noise. Indeed, electron temperatures of ~ 200 eV may be necessary in some implementations to avoid excessive collisional damping of the pump or seed during their propagation through the amplifier.

To avoid the difficulties associated with propagation of the pump it has been proposed that the relatively long (~ 1 cm) plasma amplifying medium be replaced by a neutral gas of the appropriate density to satisfy the Raman resonance condition once fully ionized.¹² If a pumping pulse of intensity below the ionization threshold for the gas is used, the pumping pulse may then be propagated through the entire amplifier without the possibility of spontaneous Raman backscatter. In conjunction with a seed pulse of intensity greater than the threshold for rapid photoionization, the gas will be completely ionized to the appropriate density only at the front of the amplifying seed pulse and allow the backscatter of the pump only in this region and so only the useful amplification of the seed. Generating the plasma *in situ* by photoionization from the seed, however, necessarily results in an added damping of the seed. For a self-ionizing Raman amplifier to be feasible, a regime must then be found for which not only is the pump well below and the seed well above the photoionization threshold, but also for which the nonlinear Raman growth rate of the seed exceeds its damping rate due to ionization or other effects. The small blueshift of the pump as it propagates into an oncoming ionization front^{13,14} would also require a slight compensation in the frequency of the pump or seed for resonance to occur in an ionizing plasma.

Total output laser intensities of $\sim 10^{17}$ W/cm² for 0.5 μ m radiation are found to be feasible for such a scheme using a pump of 10^{13} W/cm² and a seed of 5×10^{14} W/cm² over an amplification length of 5.6 cm in hydrogen gas. This is to be compared with amplification to an equivalent output intensity in a preionized plasma of length 0.35 cm by a pump of 10^{15} W/cm². In effect, the higher pump intensity tolerable for a plasma is traded for a longer but stabler interaction length in a neutral gas to obtain identical output intensities. An experimental arrangement similar to that of Ref. 15 can be imagined using focused spot sizes of ~ 50 μ m in a gas of density 2.3×10^{17} cm⁻³ but with much higher seed intensities.

Even if spontaneous pump backscatter from noise in a pre-ionized plasma ultimately proves not to be a difficulty for the conventional amplification scheme, a self-ionizing

amplifier appears still to have the advantage of simplicity. While the conventional amplifier requires the preparation (and temporary maintenance) of a plasma of a specific density, and possibly density gradient, and that the plasma be heated to $T_e \sim 200$ eV, a self-ionizing amplifier requires only the far simpler arrangement of an amplifying chamber filled with gas to a specified uniform density. Overall, the far lower fluctuation levels and simpler handling properties of a gaseous as opposed to plasma medium suggest that a self-ionizing amplifier may well be favored simply from practical considerations. In addition, precursor pulses, which may disrupt backward Raman amplification in a pre-ionized plasma,¹⁶ can be eliminated due to the absence of plasma ahead of the seed pulse front.

Note that the method contemplated here is pulse compression by ionization-induced backscatter of the pump, with the ionization induced by the backscattered pulse, which is much more intense than the pump. There are other ionization effects which induce pulse shortening, primarily the erosion of the leading edge of the pulse.¹⁷ These effects, however, apply to high intensity femtosecond pulses traveling through ionizing plasma in the absence of a counterpropagating pump wave.

This paper demonstrates a regime in which an ionization front may be employed for coupling the pump to an amplifying seed pulse. Conditions on the pump intensity, laser polarization, working gas, and other parameters are quantified and the most favorable regime for self-ionizing amplification identified. This paper is organized as follows: Sec. II describes the effects and governing equations used in modeling a self-ionizing Raman amplifier. Section III describes the energetics of pulse amplification and plasma ionization which represent constraints on the possible regimes of operation for a self-ionizing Raman amplifier. Section IV presents a numerically calculated example of self-ionizing amplification and an example of how the disrupting effect of precursor pulses can be avoided in self-ionizing amplification. Section V offers concluding remarks and possibilities for further research.

II. MODEL OF A SELF-IONIZING RAMAN AMPLIFIER

The envelope approximation (see, e.g., Ref. 18) in one dimension is used to model the Raman backscatter interaction¹⁹ in which the two light waves (1,2) are coupled by the Langmuir wave (3) according to the equations,

$$\begin{aligned}(\partial_t - v_1 \partial_x + \nu_1/2)a_1 &= K a_2 a_3, \\ (\partial_t - v_2 \partial_x + \nu_2/2)a_2 &= -K a_1 a_3^*, \\ (\partial_t - v_3 \partial_x + \nu_3/2)a_3 &= -K a_1 a_2^*.\end{aligned}\quad (1)$$

Here a_i is the potential envelope of each wave normalized to $m_e c^2/e$ for the light waves and $(\omega_{pe}/2\omega)$ ($m_e c^2/e$) for the Langmuir wave, v_i is the corresponding wave group velocity, and ν_i the wave energy damping rate taking into account the effects of inverse Bremsstrahlung when $v_{osc} \gg v_{te}$.²⁰ The wave coupling parameter K is $(n_e/n_c)^{1/4}/\sqrt{2}$ for circular polarization and $(n_e/n_c)^{1/4}/2$ for linear polarization with n_e the electron density and $n_c \doteq m_e \omega^2/4\pi|e|^2$ the critical density

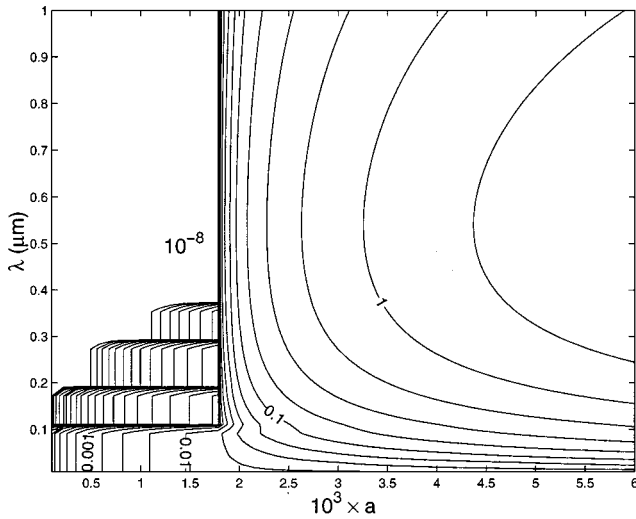


FIG. 1. Logarithmically spaced isocontours of the composite ionization probability $w(a, \lambda)/\omega$ for hydrogen and circularly polarized light.

corresponding to the laser frequency. It is assumed that the plasma is sufficiently rarefied ($n_e/n_c \ll 1$) that the laser frequencies are approximately comparable $\omega_1 \approx \omega_2 \equiv \omega \gg \omega_3 \equiv \omega_p$ in Eq. (1) and that the laser phase velocities are both approximately the velocity of light in vacuum. Since the pulse length is always much greater than the plasma wavelength in the Raman amplification regime, Eqs. (1) should remain valid throughout the amplification process provided wave breaking is avoided and there should be no added damping of the seed due to formation of a plasma wake.

The photoionization rate of an atomic gas in an intense laser field can be modeled by the Keldysh formula^{21,22} provided $E \ll m_e^2 |e| \hbar^4$, or equivalently $a \ll m_e |e| \hbar^4 \omega c \approx 0.1$ for half-micron radiation.²³ For small electric fields, $\gamma \doteq \sqrt{2U_I/m_e c^2}/a \gg 1$, a multiphoton formula for the ionization rate applies,

$$w(a) \approx \omega N^{3/2} (2\gamma)^{-2N}, \quad (2)$$

where $w(a)$ is the probability of ionizing a single neutral atom per unit time, U_I is the ionization potential, and $N \doteq 1 + \text{Int}(U_I/\hbar\omega)$ is the number of photons required to overcome that potential. For large electric fields, $\gamma \ll 1$, a tunneling formula is accurate,

$$w(a) \approx 4 \Omega_0 \left(\frac{U_I}{U_H} \right)^{5/2} \frac{a_H}{a} \exp \left[-\frac{2}{3} \left(\frac{U_I}{U_H} \right)^{3/2} \frac{a_H}{a} \right], \quad (3)$$

where U_H is the ionization potential of hydrogen, $\Omega_0 \doteq \alpha c/r_{\text{Bohr}} \approx 4.1 \times 10^{16} \text{ s}^{-1}$ is the ‘‘atomic frequency,’’ and $a_H \approx 3.05 \times 10^{14}/\omega (\text{s}^{-1})$ the normalized vector potential associated with the hydrogenic electric field. The cycle averaged form of Eq. (3) is necessary for linear polarization. In the small region between the multiphoton and tunneling regimes a simple linear interpolation between Eqs. (2) and (3) is used. For $a \sim m_e |e| \hbar^4 \omega c$ (beyond the validity range of the Keldysh model), the ionization rate is so rapid that all of the available gas may be treated as ionized instantaneously on the time scale of the laser period.

Figure 1 shows logarithmically spaced iso-contours of

the composite ionization probability as a function of laser wavelength λ and amplitude a for atomic hydrogen and circularly polarized light. A window of low ionization probability ($w/\omega \leq 10^{-8}$), suitable for propagating the pumping beam over some distance, is evident for $a \leq 0.002$ and $\lambda \geq 0.2 \mu\text{m}$ (corresponding to $I \sim 10^{13} \text{ W/cm}^2$), and threshold behavior is seen near $a \approx 0.002$ over the span of wavelengths $\lambda = 0.2\text{--}1.0 \mu\text{m}$. Above $a \approx 0.005$ ($I \sim 10^{14} \text{ W/cm}^2$), the ionization rate is effectively instantaneous for $\lambda = 0.2\text{--}1.0 \mu\text{m}$ marking a lower limit for the seed amplitude in a self-ionizing amplifier. These thresholds are on the order of the values cited for helium in Ref. 24.

Due to photoionization, the electron and neutral densities evolve according to the equations,

$$\partial_t n_e = n_n w(a) \quad \text{and} \quad \partial_t n_n = -n_n w(a). \quad (4)$$

By energy conservation, the wave fields must also damp according to

$$n_c \frac{m_e c^2}{2} \partial_t |a|^2 = -(U_I + \langle \varepsilon \rangle) \partial_t n_e, \quad (5)$$

where $|a|^2 \doteq a_1^2 + a_2^2 + \frac{1}{2} \sqrt{(n_e/n_c)} a_3^2$ and $\langle \varepsilon \rangle$ represents the average energy acquired by an electron born in the laser field of magnitude $a(x, t)$. This equation corresponds to the ‘‘nonadiabatic’’ losses due to ionization as discussed in Ref. 25. For multielectron atoms, the effect of second, third, etc., ionizations results in additional damping. The far slower process of recombination is completely negligible for the short time scales applicable to Raman amplification. Scattering to other wavelengths due to ionization is also neglected.

The average electron birth energy is given by

$$\langle \varepsilon \rangle \doteq \frac{1}{N} \int_0^\infty d\varepsilon f(\varepsilon) \varepsilon \quad \text{with} \quad N \doteq \int_0^\infty d\varepsilon f(\varepsilon),$$

where $f(\varepsilon)$ is the electron distribution function in the wake of the ionizing pulse corresponding to electron birth in the given total electric field $a(x, t)$. Note that the instantaneous electric field $a(x, t)$ at the position and time of an electron's birth determines its contribution to the residual oscillation energy $\langle \varepsilon \rangle$. Though the electron oscillates in any subsequent field, only the drift energy imparted to it at the time of ionization (determined by the phase of the electric field) remains with the electron and contributes to the ionization damping of the laser field.

For the case of linear polarization, using the conservation of each electron's transverse canonical momentum $\mathbf{p} - |e|\mathbf{A}/c$ with \mathbf{A} the laser vector potential, the energy distribution of electrons left behind by an ionizing laser pulse (considering only the simple case of hydrogen from which one electron is liberated) may be calculated²⁶ from Eq. (3) to be

$$f(\varepsilon) = \frac{1}{\varepsilon_{\text{osc}}} \left(1 - \frac{\varepsilon}{\varepsilon_{\text{osc}}} \right)^{-1} \left(\frac{\varepsilon}{\varepsilon_{\text{osc}}} \right)^{-1/2} \times \exp \left[-\beta \left(1 - \frac{\varepsilon}{\varepsilon_{\text{osc}}} \right)^{-1/2} \right] \Theta(2\varepsilon_{\text{osc}} - \varepsilon), \quad (6)$$

where $\epsilon_{osc} \doteq m_e c^2 a^2 / 4$ is the time averaged oscillation energy of the laser field at the time of ionization, $\beta \doteq (2/3) \times (U_I / U_H)^{3/2} (a_H / a)$, and $\Theta(x)$ is the unit step function.

For atomic hydrogen with $U_I \approx 13.6$ eV, $\lambda \approx 0.5$ μm , and $a \sim 0.01 - 0.001$, then $\beta \sim 5 - 50 \gg 1$ and the integral may be evaluated asymptotically to yield

$$\langle \epsilon \rangle \sim \sqrt{2\pi} \frac{\epsilon_{osc}}{K_0(\beta)} \beta^{-3/2} e^{-\beta} \sim \frac{m_e v_{osc}^2}{2\beta}, \quad \beta \rightarrow \infty, \quad (7)$$

where use is made of the large argument approximation for the modified Bessel function $K_0(\beta) \sim \sqrt{\pi/2\beta} e^{-\beta}$.²⁷ At sufficiently large a , β is no longer large and the approximation of Eq. (7) no longer applies; however, this results only in an overestimate of $\langle \epsilon \rangle$ and, at worst, a conservative estimate of the cost of the ionization damping.

In contrast, for circular polarization, the constancy of the magnitude of the electric field results in a distribution peaked near the laser oscillation energy,²⁸ so that $\langle \epsilon \rangle \sim m_e v_{osc}^2 / 2$. Consequently, for large β , linear polarization results in a substantially reduced contribution of the oscillation energy to the ionization damping rate relative to circular polarization. In both cases, the energy left in the longitudinal oscillations of the Langmuir wake of the ionizing pulse²⁹ are of order a_2^2 relative to transverse oscillation energy and hence negligible for the parameter regime of interest.

III. ENERGETICS OF SELF-IONIZING RAMAN AMPLIFICATION

With these equations, an estimate of the overall limitations placed on Raman amplification due to ionization damping may be made. Assuming the seed pulse reaches the advanced nonlinear phase of amplification when significant depletion of the pump occurs, during a time interval Δt , the seed would gain an energy increment from the pump of

$$\Delta \epsilon_+ \sim 2 c \Delta t \epsilon \frac{E_1^2}{8\pi} \sim 2 c \Delta t \epsilon n_c \frac{m_e c^2}{2} a_1^2,$$

where $\epsilon \sim 0.8$ represents the fraction of pump depletion as calculated in Ref. 9. Simultaneously, and again for the simple case of hydrogen, the seed would lose an energy increment due to total ionization of the background gas of

$$\Delta \epsilon_- \sim c \Delta t n_n (U_I + \langle \epsilon \rangle).$$

The criterion for net amplification, $\Delta \epsilon_+ > \Delta \epsilon_-$, may then be written as

$$\frac{n_n}{n_c} < \epsilon \frac{m_e c^2}{U_I + \langle \epsilon \rangle} a_1^2. \quad (8)$$

With a_1 constrained by the ionization threshold given in Fig. 1 ($a_1 \sim 0.0015$), Eq. (8) constitutes a limitation on the acceptable precursor gas density.

An accurate estimate of the limitation placed on n_n by Eq. (8), requires an evaluation of the average electron birth energy $\langle \epsilon \rangle$ including two important effects: Foremost, an estimate of the characteristic amplitude in the seed pulse profile at which the majority of electrons are born must be made since the source of electrons n_n may be completely depleted long before the complete seed pulse passes any representa-

tive neutral atom. Electrons born in the leading part of the pulse oscillate in the high intensity fields near the peak of the seed, but ultimately return their oscillation energy to the pulse as it passes and retain only the drift energy established by the low intensity field at which they were born. Second, as shown for linearly polarized lasers, the majority of particles do not possess the full laser field oscillation velocity corresponding to the field amplitude at which they are born.

The amplitude of a_2 where the majority of electrons are born (i.e., where n_n drops rapidly in the ionizing field of the seed) may be estimated by considering the simple model (valid in the small neighborhood of the steep seed pulse front where most ionization occurs) of a laser pulse whose amplitude increases linearly with a slope η behind the pulse front, $a(x, t) = \eta(ct - x)\Theta(ct - x)$, impinging on a step-function distribution of neutral gas, $n_n(x, t = 0) = \Theta(x)$. For the case of linear polarization, integrating the second of Eqs. (4) for these conditions using the cycle averaged form of Eq. (3) and assuming $a(x, t)$ to be unperturbed by the ionization process (i.e., the case of a strong seed in a tenuous gas) gives

$$n_n(x, t) = \Theta(x) \exp \left\{ - \frac{w_0 \sqrt{\beta'}}{c \eta} \Gamma \left[- \frac{1}{2}, \frac{\beta'}{\eta(ct - x)} \right] \times \Theta(ct - x) \right\},$$

where $\beta' \doteq (2/3)(U_I / U_H)^{3/2} a_H$, $w_0 \doteq 4 \sqrt{3/\pi} \Omega_0 (U_I / U_H)^{7/4} \times \sqrt{a_H}$, and $\Gamma(a, x)$ is the incomplete Gamma function. Using the large argument expansion for $\Gamma(a, x)$,²⁷ in the region just behind the pulse front ($\beta' / \eta(ct - x) \rightarrow +\infty$),

$$n_n(x, t) \sim \Theta(x) \exp \left\{ - \frac{w_0 \sqrt{\eta}}{c \beta'} (ct - x)^{3/2} \times \exp \left[- \frac{\beta'}{\eta(ct - x)} \right] \right\}.$$

For typical parameters, the characteristic depth into the pulse at which the majority of electrons is born is then approximately found to be

$$(ct - x) \approx \frac{\beta' / \eta}{\ln(w_0 \sqrt{\beta'} / c \eta)},$$

so that the corresponding laser intensity in this linear model is then

$$a \approx \frac{\beta'}{\ln(w_0 \sqrt{\beta'} / c \eta)}.$$

In the case of circular polarization, using the unaveraged form of Eq. (3), a similar calculation (now with $w_0 \doteq 4 \Omega_0 (U_I / U_H)^{5/2} a_H$) yields for the characteristic field strength at which most electrons are born

$$a \approx \frac{\beta'}{\ln(w_0 / c \eta)}.$$

In both cases, a increases with increasing pulse steepness. Note that, for these parameters, since the cycle-averaged ionization rate appropriate for linear polarization is slightly less

than the unaveraged result applicable to circular polarization, the majority of electrons are born at a slightly higher field for linear polarization as opposed to circular polarization. However, the reduction in $\langle \varepsilon \rangle$ for linear polarization largely compensates this effect, so that the characteristic energy at which most electrons are born in a linearly polarized pulse is actually less than that for circular polarization for all values of $\eta\lambda$ for which the envelope approximation is valid.

For a typical seed pulse front with $\eta\lambda \approx 0.1$ in the nonlinear regime and again for the case of atomic hydrogen with $\lambda = 0.5 \mu\text{m}$ and $a_1 = 0.0015$, using these estimates of a in evaluating Eq. (7) (noting that β depends on a for linear polarization) and Eq. (8) leads to

$$\frac{n_n}{n_c} < \epsilon \frac{m_e c^2}{U_I + \langle \varepsilon \rangle} a_1^2 \approx 0.048.$$

For circular polarization, the amplification condition is

$$n_n/n_c < 0.023$$

for the same parameters.

In both cases, a density threshold must not be exceeded for nonlinear amplification to overcome ionization damping. Also, though for fixed a , $\langle \varepsilon \rangle$ may be significantly greater for circular polarization, the net advantage of linear polarization in terms of the ionization damping rate proves only marginal due to the dominating contribution of the ionization potential in Eq. (8) and since most electrons are born at a lower field amplitude with circular polarization for typically steep pulses.

Note that, should the allowable pump intensity prove to be lower than that given by Fig. 1 and assumed above, this should only result in the necessity of using lower gas densities in accordance with Eq. (8). However, n_n may not be reduced arbitrarily since the resultant plasma must be sufficiently dense to prevent the breaking of the backscatter-driven Langmuir wave and subsequent incomplete pump depletion. Using the wave breaking criterion $\omega_p > \omega_b \doteq \sqrt{|e|k_3 E_3/m_e}$ and the Manely–Rowe relation $a_1^{\text{max}} \sim a_3^{\text{max}}$ with $k_3 \approx 2\omega/c$ gives $a_1 \leq (\omega_p/\omega)^{3/2}/\sqrt{2}$ or $n_n/n_c \geq 2^{3/2} a_1^{4/3}$ to avoid breaking. The composite criterion on the neutral density may then be written

$$2^{3/2} a_1^{4/3} \approx 0.00027 < \frac{n_n}{n_c} < \epsilon \frac{m_e c^2}{U_I + \langle \varepsilon \rangle} a_1^2 \approx \begin{cases} 0.048, & \text{linear polarization} \\ 0.023, & \text{circular polarization.} \end{cases} \quad (9)$$

To within the order unity accuracy to be expected of the above estimates, these limits were observed to be generally consistent with results found numerically (see Sec. IV). For circular and linear polarizations, peak seed amplitudes were observed to stabilize at little more than their initial amplitudes $a_2 \sim 0.01$ (although pulse shapes would sharply steepen as an effect of the ionization front) for $n_n = 0.01 n_c$. A gas density of $n_n \leq 0.002 n_c$ was found necessary for substantial amplification of the seed to $a_2 \geq 0.1$.

A threshold also applies for the amplitude and steepness of the seed pulse for a self-ionizing amplifier to be feasible.

In contrast to the pump, constraints on the seed arise from the complex spatiotemporal evolution of an initial pulse through the linear pulse broadening regime into the nonlinear pump depletion regime, including ionization damping, and do not appear amenable to simple arguments of the type used to estimate the pump threshold. The initial seed pulse must be sufficiently intense and the linear Raman growth rate (dependent on a_1 and n_e) sufficiently rapid that the linear response, growing exponentially in the fully ionized plasma behind the seed, replenishes the seed pulse before the seed intensity is damped below the threshold for rapid ionization. Neglecting ionization damping, the condition for the seed to access the nonlinear regime can be quantified as the seed pulse length L_{seed} exceeding the Raman growth length in the seed $c/a_2 \sqrt{\omega \omega_p}/2$ or $a_2 > \sqrt{2} n_c/n_n / (kL_{\text{seed}})$. For a 1 ps initial seed, a minimum seed intensity (i.e., ignoring ionization) is then $a_2 > 0.002$ for the same parameters as above.

Numerically, at the threshold density of $n_e = 0.01 n_c$, seed amplitudes of $a_2 \geq 0.008$ and 0.01 for circular and linear polarizations, respectively (comparable to the requirement for rapid ionization) were found necessary merely to ensure sustainment of the seed at its initial intensity in the face of ionization. In this regime of relatively gentle pulse fronts where the ionization damping rate for linear polarization slightly exceeds that for circular polarization and since the wave coupling constant K and hence linear Raman growth rate is slightly larger for circular polarization, circular polarization is evidently favored. Similarly, and since linear polarization results in only a slight reduction in ionization damping for the nonlinear regime, circularly polarized fields are also seen to reach slightly higher final amplitudes. In addition, the collisional damping rate for circularly polarized pulses is less than that for linear polarization due to the presence of stagnation points in electron orbits in linearly polarized fields.

Combining the first of Eqs. (4) with Eq. (5) shows that the wave energy damping from ionization scales as n_n/n_c . Since the linear Raman growth rate scales as $a_1 K \sim a_1 (n_e/n_c)^{1/4} \sim a_1 (n_n/n_c)^{1/4}$, for any fixed a_1 , the growth rate during the crucial linear phase may then always be arranged to exceed the ionization damping by sufficiently reducing n_n . Reducing the linear wave coupling incurs the cost of a longer interaction length to access the nonlinear regime; however, provided the lower bound due to wave breaking is not crossed, the only limit to this process is that imposed by the physically allowable size of a practical device and associated optics.

Within the model of Eqs. (1), the attainable amplitude of a_2 is constrained only due to steepening of the pulse front during the amplification process and consequent increase of the characteristic $\langle \varepsilon \rangle$. Such a limit is generally reached only beyond the validity of Eqs. (1), however. Beyond the approximations of Eqs. (1), in the conventional Raman amplification scheme, the total amplification process is expected to be limited by either Raman forward scattering or modulational instabilities of the highly amplified seed to times less than $T_{\text{amp}} \sim 1/\omega_p a_1^{4/3}$. Maximizing T_{amp} by minimizing ω_p subject to the constraint that $\omega_p \geq \omega(4a_1)^{2/3}$ to avoid Langmuir wave-breaking and incomplete pump depletion gives a

TABLE I. Example output parameters.

| λ (μm) | 0.2 | 0.5 | 1.0 |
|--|----------------------|----------------------|----------------------|
| n_e/n_c | 0.001 | 0.001 | 0.001 |
| $L_{\text{amp}}(\text{cm}) \sim \lambda(\text{cm})/4a_1^2$ | 2.22 | 5.55 | 11.1 |
| $a_{2,\text{out}} \sim 1.2a_1^{1/3}$ | 0.14 | 0.14 | 0.14 |
| $T_{\text{out}}(\text{fs}) \sim 1.3\lambda(\mu\text{m})/a_1^{2/3}$ | 49.6 | 124 | 248 |
| $I_{\text{out}}(\text{W}/\text{cm}^2) \sim 4 \times 10^{10} \epsilon a_1^{2/3}/\lambda(\text{cm})^2$ | 1.3×10^{18} | 2.1×10^{17} | 5.2×10^{16} |

maximum amplification length of $L_{\text{amp}} \sim \lambda/a_1^2$. Also using the limit $\omega_p \sim \omega(4a_1)^{2/3}$, the output pulse temporal length is of order $T_{\text{out}}(\text{fs}) \sim 6/\omega_p \sim 1.3\lambda(\mu\text{m})/a_1^{2/3}$, so that the output pulse peak intensity for linear polarization is $I_{\text{out}}(\text{W}/\text{cm}^2) \sim \epsilon L_{\text{amp}} E_1^2/8\pi c T_{\text{out}} \sim 4 \times 10^{10} \epsilon a_1^{2/3}/\lambda(\text{cm})^2$ and its amplitude $a_{2,\text{out}} \sim [I_{\text{out}} \lambda^2(\text{W})/1.37 \times 10^{10}]^{1/2} \sim 1.7 \epsilon^{1/2} a_1^{1/3}$.

As shown above, self-ionization, in addition to constraining the pump to intensities less than the threshold for significant ionization, stipulates a range of acceptable gas densities. In the region of parameter space where these constraints are satisfied, and assuming self-ionizing amplification to be limited by forward Raman or modulational instabilities as in the conventional case, the output pulse parameters may be calculated by the above formulas. Here it is also assumed that ionization damping introduces only an order unity multiplier to the energy gained by the seed from the pump (i.e., a fixed, small fraction of pump energy transferred to the seed must be diverted for ionization during any time interval) and hence does not effect the power scaling. Example parameters for a self-ionizing amplifier using atomic hydrogen with $a_1 = 0.0015$ are summarized in Table I. All appear to be within the constraints of a practically realizable device.

Note that, for a three-dimensional experimental arrangement, as the pump beam comes to a focus, the maximum pump intensity cannot be allowed to exceed the ionization threshold of the working gas. At some point, the wings and tail of the beam will also fall below the intensity required to satisfy Eq. (8) for a fixed gas density. Unless the distance of this point from the focal point can be arranged to exceed L_{amp} above, an additional limit will be placed on the maximum achievable intensity. Similarly, only the peaked, central portion of the seed pulse will substantially exceed the photoionization threshold and be amplified while the transverse wings of the pulse are damped. Longitudinally, the focusing of the seed intensity will require the seed intensity already to exceed the ionization threshold before entering the region where the pump intensity satisfies Eq. (8), again constraining the optics of the system. If the seed is amplified as it is focusing, then these effects may be ignorable; and in general, these constraints will depend on a particular experimental setup. The overall degree of pump depletion can be expected to be similar in three dimensions as it is in one, namely, $\epsilon \sim 0.8$.

The above calculations have been for the simple, mono-electronic case of hydrogen. The somewhat higher first ionization potential of helium, however, makes this gas more desirable as an amplifying medium since it could sustain higher pump intensities without ionization, but its second

electron complicates the energy arguments given above for hydrogen. Simply approximating the oscillation energies $\langle \epsilon_i \rangle$ of each electron liberated from helium as being of the order of the corresponding ionization potential U_i (an overestimate) and since helium can withstand pump intensities of $a_1 \sim 0.002$ without ionizing leads to the conditions

$$2^{3/2} a_1^{4/3} \approx 0.00071 < 2 \frac{n_n}{n_c} < \epsilon \frac{m_e c^2}{2(U_1 + U_2)} a_1^2 \approx 0.0052,$$

$$L_{\text{amp}} \sim \frac{\lambda}{4a_1^2} \sim 3.13 \text{ cm},$$

$$I_{\text{out}} \sim 4 \times 10^{10} \epsilon \frac{a_1^{2/3}}{\lambda^2} \sim 2.5 \times 10^{17} \text{ W}/\text{cm}^2$$

for $\lambda = 0.5 \mu\text{m}$.

Since no gas has a higher first ionization potential than helium, a helium medium permits the highest pump intensities for a self-ionizing amplifier and hence (by the scalings above) accesses the highest intensities in the shortest possible distance. The relatively high first and second ionization potentials of helium, however, necessitate that only rather intense initial seeds ($a_2 \sim 0.05$), able to survive the initial ionization damping before the nonlinear state is reached, can be used. The situation is exacerbated for atoms with three or more electrons. In contrast, while hydrogen can support a pump strength of only $a_1 \sim 0.0015$, its single electron requires only an initial $a_2 \sim 0.01$. Hence, hydrogen affords the greatest possible relative amplification factor (output amplitude relative to initial seed amplitude) of any gas.

IV. EXAMPLES OF SELF-IONIZING AMPLIFICATION

With the assumptions discussed above, Eqs. (1), (4), and (5) have been integrated numerically in the frame of the seed pulse. Figure 2 gives an example comparison of the time evolution of identical seed pulses of $a_2(t=0) = 0.01$ and $\lambda = 0.5 \mu\text{m}$ amplified by a pump of $a_1 = 0.0015$ in a pre-ionized plasma of $n_e = 0.001 n_c$ and $T_e = 500 \text{ eV}$ and in an ionizing hydrogen gas of equivalent density. In both cases, the lasers are circularly polarized.

In the pre-ionized case, the characteristic “ π -pulse” shape of the nonlinear regime of amplification is evident subject to modifications due to slight collisional damping. The peak amplitude of the leading spike is seen to grow linearly with time, while the pulse width decreases inversely with time. A total peak power amplification by a factor of ~ 200 , corresponding to an output intensity of $2.1 \times 10^{17} \text{ W}/\text{cm}^2$, is reached for the leading spike with an out-

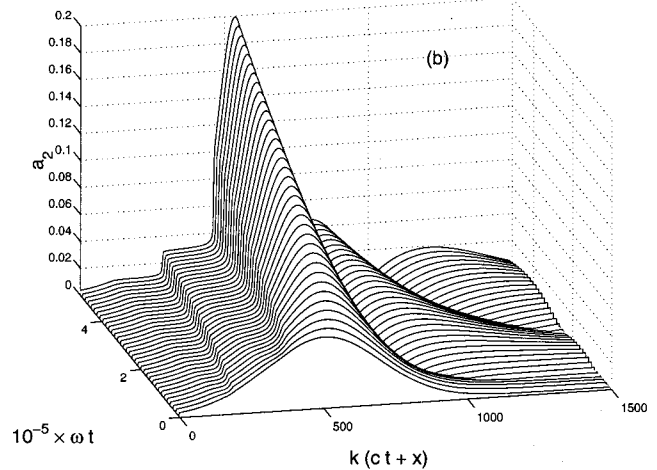
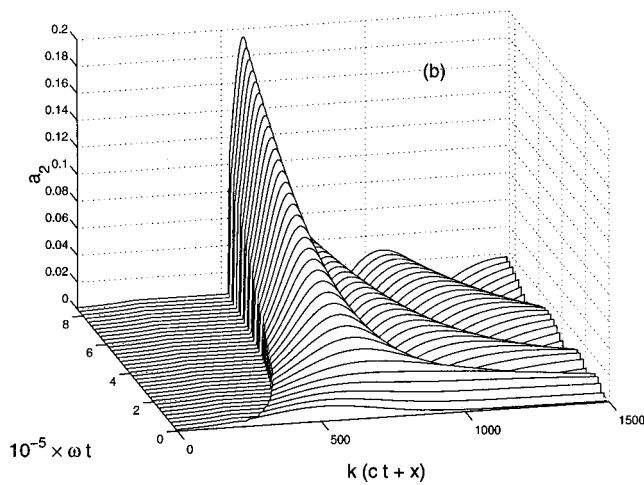
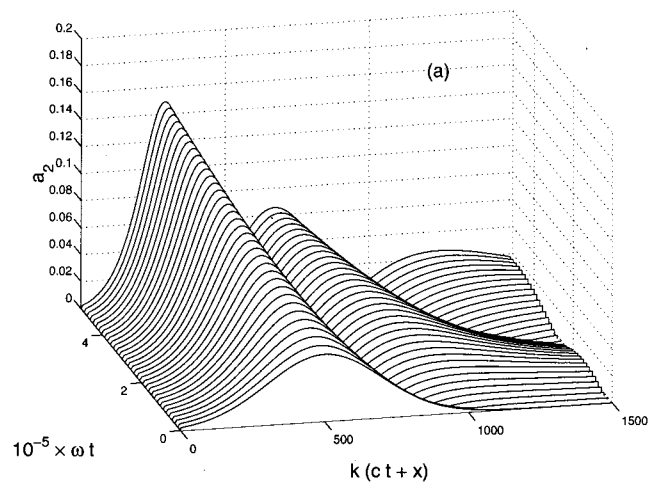
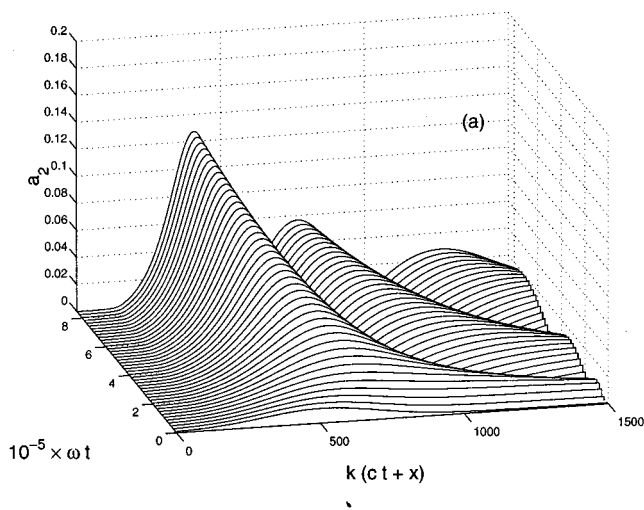


FIG. 2. Comparison of pre-ionized (a) and self-ionizing (b) Raman amplification in hydrogen with $a_1=0.0015$, $a_2(t=0)=0.01$, $n_e=0.001 n_c$, $\lambda=0.5 \mu\text{m}$, and $T_e=500 \text{ eV}$ for the pre-ionized case. Seed pulse envelopes as a function of time and distance in the pulse frame are plotted. Pump pulses (not shown) enter from the left. Polarizations are circular.

FIG. 3. Comparison of pre-ionized (a) and self-ionizing (b) Raman amplification in helium with $a_1=0.002$, $a_2(t=0)=0.05$, $n_e=0.0005 n_c$, $\lambda=0.5 \mu\text{m}$, and $T_e=500 \text{ eV}$ for the pre-ionized case. Seed pulse envelopes as a function of time and distance in the pulse frame are plotted. Pump pulses (not shown) enter from the left. Polarizations are circular.

put pulse width equivalent to one half of the input width. Beyond $a_2 \sim 0.14$, a modulational instability of the high-amplitude pulse is expected to end the amplification process.

Remarkably, the self-ionizing pulse reaches a slightly higher amplitude in the same time ($I_{\text{out}} \sim 4.0 \times 10^{17} \text{ W/cm}^2$ or amplification by a factor of ~ 360) and is slightly more compressed (~ 4 times) but is seen also to have fallen behind its analog for the pre-ionized case. This results from the combined effects of slow erosion and steepening of the pulse front in the ionization layer and that only the later part of the seed pulse where the plasma is fully ionized is amplified. The very leading edge of the seed pulse damps below the ionization threshold without being amplified and is evident in the later stages as the low amplitude foot stretching ahead of the main peak of the amplifying seed. The very steep leading edge imprinted on the seed pulse by ionization accelerates its depletion of the pump and hence its narrowing and amplification by the same mechanism as in the nonlinear

regime of the pre-ionized case.⁶ Note that both pulses evolve towards the π -pulse through similar linear regimes: a pulse broadening regime characteristic of the linearized solutions of Eqs. (1),⁸ with the addition of a notching of the initial seed pulse due to ionization damping in the ionizing case. That both reach similar asymptotic states is evidence of the π -pulse remaining the attractor solution of Eqs. (1) despite the substantial perturbation introduced by ionization effects.

Figure 3 gives an example comparison of the time evolution of identical seed pulses of $a_2(t=0)=0.05$ and $\lambda=0.5 \mu\text{m}$ amplified by a pump of $a_1=0.002$ in a pre-ionized plasma of $n_e=0.0005 n_c$ and $T_e=500 \text{ eV}$ and in an ionizing helium gas of equivalent density. Again, both lasers are circularly polarized. Here the ionizing pulse is amplified by a factor of ~ 16 , corresponding to an output intensity of $4.4 \times 10^{17} \text{ W/cm}^2$ with an output pulse width also roughly one-quarter of the input width. For the pump intensity permis-

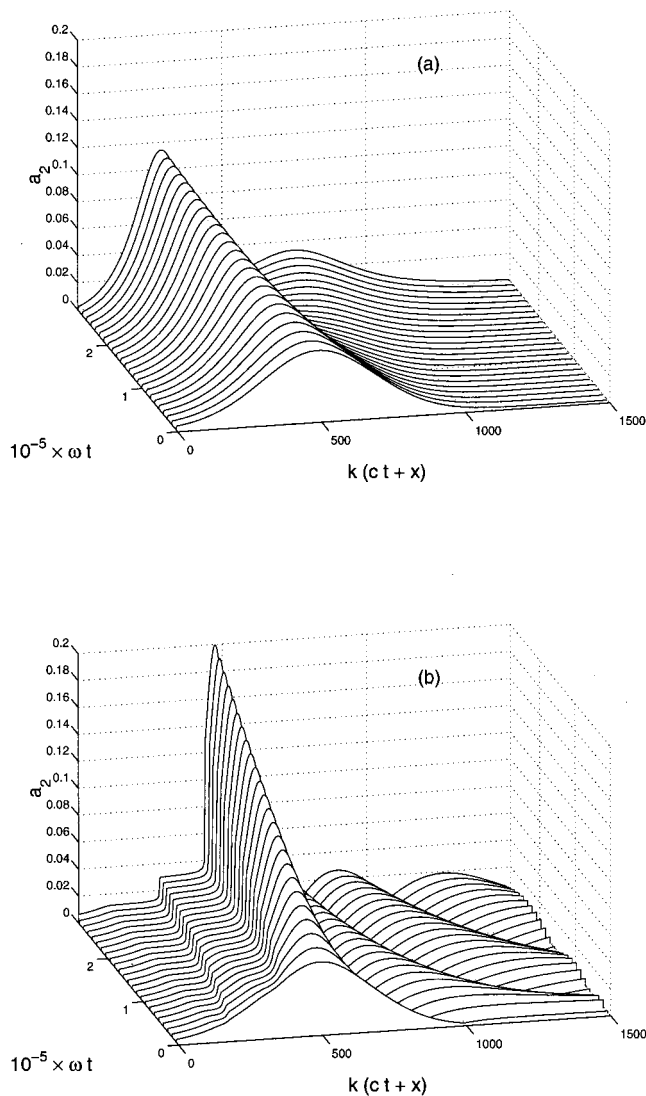


FIG. 4. Comparison of pre-ionized (a) and self-ionizing (b) Raman amplification in helium with $n_e = 0.002 n_c$ and other parameters as in Fig. 3.

sible with helium, the seed pulse is expected to be modulation-limited to $a_2 \sim 0.15$. The double notching of the seed pulse front corresponding to the two ionization states of helium is evident. The added ionization damping due to this second ionization state necessitates a much more intense initial seed so that, as mentioned above, though the peak output intensity is slightly greater for helium, the relative amplification is significantly less than that of hydrogen.

In Fig. 4, amplification in helium gas and in a pre-ionized helium plasma of equivalent density are compared for $n_e = 0.002 n_c$ and the other parameters as in Fig. 3. For these parameters, the pre-ionized case evolves towards a “ 2π -pulse” state of constant asymptotic amplitude¹⁶ in place of the amplifying and narrowing π -pulse state. In contrast, the ionization-induced steepening of the seed pulse front in the case of gaseous helium enables a π -pulse-type solution to form with the consequent narrowing and linear amplification in time. Effectively, the ionization perturbation has broadened the basin of attraction to a π -pulse.

V. CONCLUSIONS

In summary, an elementary analysis has demonstrated a regime of feasibility for a self-ionizing, plasma-based backward Raman amplifier. In the conventional Raman amplifier, instability of the pumping beam to spontaneous backscatter due to fluctuations in the preformed plasma medium may be a severe obstacle to successful amplification. By using the intense amplifying seed pulse to generate the plasma by photoionization of a neutral gas only in the region where Raman scattering is needed to occur, the instability of the pump may be avoided provided that the pump intensity is kept below the threshold for significant ionization. It has been shown that the damping rate due to photoionization by the seed may be successfully overcome by the nonlinear Raman amplification rate provided that a threshold gas density is not exceeded. In effect, with the pump amplitude determined by the ionization threshold of the working gas, a range of allowable gas densities is determined. A sufficiently intense seed is also required to photoionize the gas rapidly and to access the nonlinear regime of Raman amplification before excessive ionization damping occurs. The output parameters of a self-ionizing Raman amplifier are then expected to scale in an equivalent manner to those of the conventional Raman amplifier operated with the same pump intensity. Though the detailed kinetics of ionization in linearly and circularly polarized fields are quite different, only marginal net differences are found between these polarizations for Raman amplification, with circular polarization appearing slightly favored. Finally, both hydrogen and helium are considered as working gases with helium affording the highest output intensity and hydrogen the greatest relative amplification factor. No advantage is gained from gases of higher atomic number.

Note that, in addition to the Raman pulse compression regime considered here, a similar effect might accompany pulse compression in the so-called Compton scattering regime, where backscattering might occur due to electron trapping effects rather than through a resonant three-wave interaction.³⁰ The self-ionizing backscatter effect, if it occurs for the Compton regime, could then be addressed by an approach similar to the one employed here for the Raman regime.

The preceding analysis has entailed many simplifications. Foremost, while self-ionization avoids instabilities resulting from the propagation of the pump beam through plasma, instabilities which might be introduced due to the sharp ionization front have not been addressed in this analysis. Specifically, an instability involving transverse modulations of the ionization front due to the nonlinearity of Eq. (3) has been identified.³¹ If the exponentiation length for such an instability proves to be less than that of the relativistic modulational instability cited above, then a new limiting constraint on the total allowable amplification length (and hence output intensity) applies. Regardless, simply initializing the seed with a higher intensity (perhaps from a previous Raman amplifier) and amplifying it over a shorter length could still result in the same output power as if a smaller initial seed

were amplified over a longer length in the absence of the instability.

The study of the growth and importance of this instability in the presence of Raman amplification requires further simulations in two dimensions which are beyond the scope of this paper. Multidimensional simulations will also allow the study of effects associated with finite focusing lengths or transverse plasma or laser field intensity gradients, etc.

The validity of the envelope approximation in Eqs. (1) becomes uncertain when extremely steep gradients in wave intensities, as results from the ionization front, appear. The exact behavior of the electron distribution created by such a rapidly changing pulse may similarly be more subtle than is captured in the ionization damping rate estimate used here. The result cited in Eq. (6) is strictly valid only for the case of adiabatic laser pulse shapes and not those with extremely steep fronts. In treating the sharp ionization front, no attempt was further made to treat realistically the Raman resonance condition for such an inhomogeneous plasma. Finally, the complicating effects of harmonic generation,³² ionization-induced blueshifting,^{33,34} or forward Raman scattering of the seed pulse in an ionizing plasma have similarly not been included. In principle, all of these issues can be addressed by PIC simulation.

ACKNOWLEDGMENTS

The authors thank E. J. Valeo, S. Brunner, and V. M. Malkin for useful discussions. The authors thank Yu. Tsidulko for suggesting the algorithm used in integrating Eqs. (1).

This work was supported by the U.S. Department of Energy under Contract No. DE-AC02-76-CHO-3073 and No. DE-FG02-97ER54436, and the Defense Advanced Research Projects Agency (DARPA).

¹J. D. Lindl, *Inertial Confinement Fusion: The Quest for Ignition and Energy Gain Using Indirect Drive* (American Institute of Physics, New York, 1998).

²E. Esarey, P. Sprangle, J. Krall, and A. Ting, *IEEE Trans. Plasma Sci.* **24**, 252 (1996).

³C. Bula, K. T. McDonald, E. J. Prebys *et al.*, *Phys. Rev. Lett.* **76**, 3116 (1996).

⁴G. A. Mourou, C. P. J. Barty, and M. D. Perry, *Phys. Today* **51** (1), 22 (1998).

⁵M. Tabak, J. Hammer, M. E. Glinsky, W. L. Kruer, S. C. Wilks, J. Woodworth, E. M. Campbell, and M. D. Perry, *Phys. Plasmas* **1**, 1626 (1994).

⁶V. M. Malkin, G. Shvets, and N. J. Fisch, *Phys. Rev. Lett.* **82**, 4448 (1999).

⁷V. M. Malkin, G. Shvets, and N. J. Fisch, *Phys. Rev. Lett.* **84**, 1208 (2000).

⁸B. L. Bobroff and H. A. Haus, *J. Appl. Phys.* **38**, 390 (1967).

⁹V. M. Malkin, G. Shvets, and N. J. Fisch, *Phys. Plasmas* **7**, 2232 (2000).

¹⁰A. B. Langdon and B. F. Lasinski, in *Methods in Computational Physics*, edited by J. Killeen, R. Alder, S. Fernbach, and M. Rotenberg, *Advances in Research and Applications* (Academic, New York, 1976), Vol. 16, p. 327.

¹¹A. B. Langdon, *J. Comput. Phys.* **30**, 202 (1979).

¹²V. M. Malkin and N. J. Fisch, *Phys. Plasmas* **8**, 4698 (2001).

¹³M. Lampe, E. Ott, and J. H. Walker, *Phys. Fluids* **21**, 42 (1978).

¹⁴W. B. Mori, *Phys. Rev. A* **44**, 5118 (1991).

¹⁵Y. Ping, I. Geltner, S. Suckewer, N. J. Fisch, and G. Shvets, *Phys. Rev. E* **62**, R4532 (2000).

¹⁶Y. A. Tsidulko, V. M. Malkin, and N. J. Fisch, "Suppression of superluminescent precursors in high power backward Raman amplifiers," *Phys. Rev. Lett.* (to be published).

¹⁷S. P. Nikitin, Y. Li, T. M. Antonsen, and H. M. Milchberg, *Opt. Commun.* **157**, 139 (1998).

¹⁸A. Bers, in *Plasma Physics*, edited by C. DeWitt and J. Peyraud, *Université de Grenoble, Summer School of Theoretical Physics, Les Houches* (Gordon and Breach, New York, 1972), p. 113.

¹⁹W. L. Kruer, *The Physics of Laser Plasma Interactions* (Addison-Wesley, New York, 1988).

²⁰G. J. Pert, *Phys. Rev. E* **51**, 4778 (1995).

²¹P. Sprangle, E. Esarey, and J. Krall, *Phys. Rev. E* **54**, 4211 (1996).

²²L. V. Keldysh, *Sov. Phys. JETP* **20**, 1307 (1965).

²³L. D. Landau and E. M. Lifshitz, *Quantum Mechanics: Nonrelativistic Theory* (Pergamon, Oxford, 1977).

²⁴T. P. Hughes, *Plasmas and Laser Light* (Adam Hilger, Bristol, England, 1975).

²⁵N. E. Andreev, M. E. Veisman, M. G. Cadjan, and M. V. Chegotov, *Plasma Phys. Rep.* **26**, 947 (2000).

²⁶N. H. Burnett and P. B. Corkum, *J. Opt. Soc. Am. B* **6**, 1195 (1989).

²⁷M. Abramowitz and I. A. Stegun, *Handbook of Mathematical Functions* (Wiley, New York, 1984).

²⁸P. B. Corkum, N. H. Burnett, and F. Brunel, *Phys. Rev. Lett.* **62**, 1259 (1989).

²⁹W. B. Mori and T. Katsouleas, *Phys. Rev. Lett.* **69**, 3495 (1992).

³⁰G. Shvets, N. J. Fisch, A. Pukhov, and J. Meyer-ter-Vehn, *Phys. Rev. Lett.* **81**, 4879 (1998).

³¹T. M. Antonsen and Z. Bian, *Phys. Rev. Lett.* **82**, 3617 (1999).

³²W. P. Leemans, C. E. Clayton, W. B. Mori, K. A. Marsh, P. K. Kaw, A. Dyson, C. Joshi, and J. M. Wallace, *Phys. Rev. A* **46**, 1091 (1992).

³³E. Esarey, G. Joyce, and P. Sprangle, *Phys. Rev. A* **44**, 3908 (1991).

³⁴S. C. Rae and K. Burnett, *Phys. Rev. A* **46**, 1084 (1992).